PET Brain imaging of α7-nAChR with [^{18}F]ASEM

Reproducibility, occupancy, receptor density, and changes in schizophrenia

Dean F. Wong, MD, PhD[1,2,3,4,11], Hiroto Kuwabara MD, PhD[1], Andrew G. Horti, PhD[1], Joshua Roberts, PhD[1], Ayon Nandi, MS[1], Nicola Casella, MD[8], James Brasic MD, MS[1], , Elise Weerts, PhD[2], Kelly Kitzmiller, BA[1], Jenny A. Phan, MBBS[1,6,7], Lorena Gapasin, MS[1], Akira Sawa, MD, PhD[2], Heather Valentine, BS[1], Gary Wand, MD[2,5], Noble George, MD[1], Michael McDonald, MD, PhD[1], William Kem, PhD[9], Robert Freedman MD[10], Albert Gjedde, MD, DSc[1,11]

1 Russell H Morgan Department of Radiology and Radiological Sciences, Johns Hopkins University School of Medicine, Baltimore, MD

2 Department of Psychiatry and Behavioral Sciences, Johns Hopkins University School of Medicine, Baltimore, MD

3 Solomon Snyder Department of Neuroscience, Johns Hopkins University School of Medicine, Baltimore, MD

4 Department of Neurology, Johns Hopkins University School of Medicine, Baltimore, MD

5 Department of Medicine, Johns Hopkins University School of Medicine, Baltimore, MD

6 Department of Biomedicine, Aarhus University, Aarhus, Denmark

7 Department of Nuclear Medicine and PET centre, Aarhus University Hospital, Aarhus, Denmark

8 Sheppard-Pratt Hospital, Baltimore , MD

9 Department of Pharmacology and Therapeutics, University of Florida, Gainesville, FL

10 Department of Psychiatry, University of Colorado, Aurora Co.

11 Department of Nuclear Medicine, University of Southern Denmark, Denmark

Abstract

The α7 nicotinic acetylcholine receptor (nAChR) increasingly has been implicated in normal brain physiology, as well as in neuropsychiatric disorders. The α7-nAChR primarily is located in cerebral cortex and sub-cortical regions, compared to the α4β2 nAChR subtype that has a more subcortical distribution. The highly cortical distribution suggests a role of α7-nAChR in cognition. We expanded the first-in-human PET imaging of α7-nAChR with [^{18}F]ASEM from five to 21 healthy non-smoking volunteers and added preliminary evidence of binding in six male patients with schizophrenia. Study aims included 1) confirmation of test-retest reproducibility of [^{18}F]ASEM binding in normal volunteers, 2) demonstration of specificity of [^{18}F]ASEM binding by competition with DMXB-A, an α7-nAChR partial agonist previously tested in clinical trials of patients with schizophrenia, 3) estimation of [^{18}F]ASEM binding potentials and α7-nAChR density in vivo in humans, and 4) α7-nAChR binding in patients with schizophrenia compared to healthy volunteers.

Test-retest PET confirmed reproducibility (>90%) (variability ≤ 7%) of [^{18}F]ASEM volume of distribution (V_T) estimates in healthy volunteers. Repeated sessions of PET in five healthy subjects included baseline and effect of inhibition after oral administration of 150 mg DMXB-A. From reduction of binding potentials, we estimated the dose-dependent occupancy of α7-nAChR by DMXB-A at 17-49% for plasma concentrations at 60-200 nM DMXB-A. In agreement with evidence post-mortem, α7-nAChR density (B_{max}) averaged 0.67-0.82 nM and inhibitor affinity constant (K_I) averaged 170-385 nM. Median V_T in the six patients with schizophrenia was lower than in healthy volunteers in cingulate cortex, frontal cortex, and hippocampus. Mann-Whitney test identified cingulate cortex and hippocampus as regions with significantly lower median V_T in patients than in healthy volunteers when a single outlier patient was excluded from analysis (P = 0.02, corrected for multiple comparisons).

Introduction

As ligand-gated excitatory cation channels, nicotinic acetylcholine receptors (nAChRs) in central nervous system (CNS) are fundamental to physiology (Lukas et al., 1999). The two nicotinic receptor subtypes α4β2 and α7 predominate in CNS among many other nAChR subtypes (Lukas et al., 1999; Gotti and Clementi, 2004). Nicotine binds with high affinity to α4β2-nAChR (K_I ~ 1 nM, Anderson and Arneric, 1994)) and much lower affinity to α7-nAChR (K_I ~ 6,000 – 14,000 nM, Davies et al., 1999).

The α7-nAChR subtype is associated with the pathophysiology of specific CNS diseases, including schizophrenia, drug addiction, depression, anxiety, and multiple neurodegenerative disorders (Verbois et al., 2000; Verbois et al., 2002; Woodruff-Pak and Gould, 2002; Albuquerque et al., 2009; D'Hoedt and Bertrand, 2009; Philip et al., 2010; Hoffmeister et al., 2011; Ishikawa and Hashimoto, 2011; Parri et al., 2011) and therefore is an important target of drug discovery. Multiple post-mortem studies have shown reduced α7 receptors in brain samples from patients with schizophrenia patients, suggesting a role of α7 in schizophrenia (see review by Thomsen et al. (2010)). In autoradiography of brains from patients with schizophrenia, reductions of α-[^{125}I] BTX binding to α7 were demonstrated in hippocampus, anterior cingulate cortex, and thalamic reticular nucleus (Freedman et al., 1995) but not in orbitofrontal or temporal lobes (Court et al., 1999; Marutle et al., 2001).

The α7-nAChR has emerged as a potential therapeutic target for treatment of schizophrenia (Wallace et al., 2011; AhnAllen, 2012; Geerts, 2012; Wallace and Bertrand, 2013; Young and Geyer, 2013a; Freedman, 2014b; Beinat et al., 2015). In animals, stimulation of α7 is procognitive (Young and Geyer, 2013a; Potasiewicz et al., 2017). In clinical trials with selective α7 agonists, activation of the receptor improved cognitive performance in patients with schizophrenia. Selected drugs (GTS-21, TC-5619, and EVP-6124) show some degree of cognitive improvement in trials of patients with schizophrenia, although none has yet proceeded to late phase or FDA approval. A common trend is the improvement of cognition with an inverted U-shaped dose–response curve, when increasing the dose of α7 agonist above a threshold resulted in loss of drug effect (Wallace and Bertrand, 2015; Lewis et al., 2017). The latest research has revealed a new generation of promising α7-targeting drugs (Beinat et al., 2016).

Despite the importance of the nicotinic receptor system, the physiological and pharmacological roles of specific receptor subtypes in CNS remain poorly understood (Philip et al., 2010; Ishikawa and Hashimoto, 2011; Marrero et al., 2011; Parri et al., 2011). Until recently, the lack of radioligands for quantitative emission tomography imaging of α7-nAChR in humans hampered non-invasive research of this receptor system. Many radiotracers of interest to α7-nAChR (^{11}C-CHIBA-1001 (Toyohara et al., 2009), ^{11}C-NS14492 (Ettrup et al., 2011; Magnussen et al., 2015) and others) have been tested, but most had suboptimal properties in PET of humans (see Gao et al. (2013) for review). Here, we further tested human subjects with [^{18}F]ASEM, the only α7-nAChR PET tracer available to humans with promising imaging characteristics (Gao et al., 2013b; Horti et al., 2014b; Horti, 2015; Coughlin et al., 2017; Hillmer et al., 2017; Wong et al., 2017). Objectives included 1) confirmation of test-retest reproducibility of [^{18}F]ASEM binding in brain of normal volunteers, 2) demonstration for the first time of specific binding and target engagement/occupancy in human brain of the partial agonist DMXB-A (GTS-21), 3) estimation for the first time of [^{18}F]ASEM binding potentials and α7-nAChR receptor density (B_{max}) and inhibitor affinity constant (K_I) for

human brain in vivo, and 4) preliminary evaluation of the target role of α7-nAChR in psychosis in six patients with schizophrenia.

Methods

Subjects

All studies were carried out with the approval of the Johns Hopkins Institutional Review Board, where all subjects provided written informed consent. Participants were recruited via advertisements within the metropolitan Baltimore region.

Twenty-one healthy, non-smoking control subjects (13 males and 8 females; age range: 18-52 years; means ± SD: 32.6 ± 12.4 years) volunteered for the study. In addition to baseline PET, 12 subjects had second baseline PET (test-retest), and 5 other subjects had a second PET after a single dose of DMXB-A. Only eight of the 12 subjects had successful test-retest PET due to technical problems in either test or retest in four subjects. Of the subjects, five (including two with test-retest from a previous publication by Wong et al. (2014)) were included in this study. Healthy volunteers had no psychotropic treatment history, were free of significant medical or neuropsychiatric disorder, and received no current medications. All subjects had negative urinary toxicology tests and provided carbon monoxide (CO) breath samples of < 4 ppm on the imaging day to confirm abstinence for at least 12 hours from tobacco smoking for any subjects (see additional inclusion/exclusion criteria in Supplemental material).

Six patients diagnosed with schizophrenia (aged 20-31 years; average 25.0 ± 4.3 (SD) years; all males; one smoker only) participated in the study. Volunteers with schizophrenia that met DSM-V criteria, with stable antipsychotic medication other than clozapine, were referred by collaborating psychiatrists. Subjects underwent neuropsychiatric characterization including Brief Psychiatric Rating (BPRS) scores. Demographic data for healthy controls and subjects with schizophrenia are listed in Table 1A and 1B.

One patient with schizophrenia was tested with PET [^{18}F]ASEM while chronically treated with risperidone and then retested with PET without drug for three weeks (discontinued for clinical reasons).

To address possible effects of antipsychotics administered to patients, we determined biodistribution in mice treated for five days with cohorts of placebo vs. risperidone, aripiprazole, or olanzapine, the three most common drugs in the present patient population, at doses equivalent to doses used in humans (Reagan-Shaw et al., 2008; Dawe et al., 2010; McOmish et al., 2012; Ning et al., 2017). Mice were injected IV with [^{18}F]ASEM and sacrificed after 60 minutes (detailed Methods and Figure A in Supplemental materials).

Positron Emission Tomography

All subjects underwent PET with the Siemens/CTI High-Resolution Research Tomography (HRRT: resolution <2 mm). The dynamic imaging continued for 90 minutes with the frame sequences of 4 x 15 sec, 4 x 30 sec, 3 x 60 sec, 2 x 120 sec, 5 x 240 sec, 12 x 300 sec. Each subject received a radial arterial catheter for collection of approximately 40 arterial plasma samples and subsequent HPLC metabolite detection during the 90-minute imaging session. Arterial plasma samples were drawn as rapidly as possible for the first two minutes and then every minute until 10 minutes past injection, every 2 minutes until 20 minutes past injection, and at the times 25, 30, 45, 60, 75, and 90 minutes

past injection. Metabolites were measured for the times of 2, 5, 10, 20, 30, 60, and 90 minutes post injection. (See Supplemental data for HPLC methods)

Each subject received 13.8 mCi ±0.23 SEM [^{18}F]ASEM synthesized by the method of Gao, et al. (2013) with average specific activity of 56,417 Ci/mmol). There were no significant differences in injected radioactivity or specific activity between the controls and patients with schizophrenia. Tracer free fraction in plasma across all subjects averaged 2.79% +/- 0.06 (SD) and was not significantly different in healthy controls and patients with schizophrenia.

Of the healthy volunteers, twelve were retested with [^{18}F]ASEM imaging approximately five weeks (mean 41.2 days) after the first PET session, including three reported by Wong et al.(2014). We carefully reviewed the radiometabolite HPLC results and elected to exclude four subjects for technical reasons (e.g., defective capture columns during early development of HPLC procedures). To determine the target engagement (occupancy) by a receptor ligand and to obtain evidence of specific binding of [^{18}F]ASEM to α7-nAChR in humans, five healthy subjects additionally underwent a second imaging session after administration of oral 150 mg of the partial agonist DMXB-A (also known as GTS21), forty minutes before the PET tracer injection. Radial arterial samples for detection of concentration DMXB-A were obtained during PET imaging at 70, 100, and 130 minutes post-dose. Concentrations of DMXB-A in subjects' plasma samples were determined quantitatively by HPLC with a modification of the previously reported method (Kem et al., 2004). (Details in supplemental information).

Menstrual phase for the women was determined by a progesterone level using levels exceeding 2 ng/ml, indicating luteal phase. For two women (one in luteal phase and one in follicular phase), menstrual phase was determined by self-reported menstrual history, as progesterone samples were not available.

PET Analysis

Volumes of interest

Volumes of interest (VOI) were selected automatically in individual subject SPGR MRI volumes using FSL (FMRIB Software Library; Jenkinson et al., 2012) FIRST tool (Patenaude et al., 2011) for subcortical regions and Freesurfer tool (Fischl et al., 2004) for cortical regions. Automated VOI were manually edited to suit the structures of interest, using a locally developed VOI tool (VOILand). Refined VOI were transferred from MRI to PET spaces according to MRI to PET coregistration parameters obtained from the coregistration module of SPM12 (Statistical Parametric Mapping; Ashburner and Friston, 2003). The VOI of PET space were applied to PET frames to obtain time-activity curves (TAC) of regions. Head-motion correction (HMC) was performed with the image co-registration module of SPM12.

Total volumes of distribution (V_T) and test-retest variability were estimated for all 21 cortical VOI (Figure 1A and B). In addition, the full VOI set was used in the calculation of dose-dependent inhibition (Figure 2), as well as for the averaged estimates of maximum binding capacity (B_{max}; Figure 3), and inhibitor affinity constant (K_I; Figure 4). For analysis of V_T differences (in patients vs. control subjects, Figure 5) and potential correlation with BPRS score (see Supplementary Material) we chose three cortical regions implicated in autoradiography with [^{125}I]α-bungarotoxin ([^{125}I]BTX)of

brain of patients with schizophrenia postmortem, previously reported with significant reductions in hippocampus (~70% , Freedman et al., 1995), frontal cortex (40%, Guan et al., 1999), and cingulate cortex (54%, Marutle et al., 2001).

Kinetic analysis

Quantification of [^{18}F]ASEM steady-state volumes of distribution (V_T) proceeded as previously published (Wong et al., 2014). Specifically, the plasma reference graphical analysis (PRGA) was used to obtain regional V_T values that served as primary outcome variable for test-retests and analyses with age, sex and neuropsychiatric testing, as well as serving as secondary outcome variable for estimates of the reference volume of non-displaceable bound radioligand (V_{ND}), competitor saturation of receptors (s), binding potentials (BP_{ND}), and receptor density (B_{max}). We completed receptor density (B_{max}) and affinity (IC_{50}, K_I) estimates of α7-nAChR in three steps in five subjects by means of DMXB-A inhibition.

We estimated the occupancy of the partial agonist inhibitor by means of estimates of the radioligand's volume of non-displaceable distributed tracer in the baseline (V_{ND}), obtained from baboon brain in vivo (Horti et al., 2014), using the conventional Inhibition Plot (IP) of Gjedde and Wong (2000). We compared the value of V_{ND} obtained from the decline of the magnitude of the total volume of V_T in in the presence of two different concentrations of SR180711, of which we used the value associated with the lower dose to avoid affecting the value of V_{ND} by changes of protein binding in brain tissue or circulation or both (see Supplemental Figure B illustrating the V_{ND} determination in baboon brain).

Applied to regional volumes of distribution (V_T), the Inhibition Plot yielded reference volumes (V_{ND}) and degrees of saturation (s), according to the equation (Phan et al., 2017),

$$V_{T(i)} = (1 - s)\, V_{T(b)} + s\, V_{ND} \qquad (1)$$

where $V_{T\,(b)}$ symbolizes the volume of distribution at baseline, $V_{T\,(i)}$ the volume at inhibition in presence of DMXB-A which competes with the radiotracer for binding to the binding site. According to Equation (1), when the regional estimates of V_T in the inhibition condition were plotted as functions of the estimates in the baseline condition, the solution yielded the reference volume, V_{ND}, and the fraction of receptors occupied by the competitive drug, s.

The initial analysis revealed V_T estimates before and after DXMB-A inhibition of similar magnitudes, compensating for values of V_{ND} that may be different in the inhibition and baseline conditions. To resolve this issue, we applied the Extended Inhibition Plot equation (EIP; (Phan et al., 2017)) that relates the radioligand distribution volumes at inhibition and baseline as follows,

$$V_{T(i)} = (1 - s)\left[\frac{V_{ND(i)}}{V_{ND(b)}}\right] V_{T(b)} + s\, V_{ND(i)} \qquad (2)$$

where values of V_{ND} at baseline and inhibition are different, denoted $V_{ND\,(b)}$ and $V_{ND\,(b)}$ at baseline and inhibition, respectively. The Extended Inhibition Plot (EIP) yielded the value of V_{ND} in the inhibition condition ($V_{ND(i)}$), when the true reference volume at baseline ($V_{ND(b)}$) is known, such that estimates yielded by EIP depend on a measure of the magnitude of the reference volume.

Volumes of distribution (V_T and V_{ND}) yielded binding potentials (BP_{ND}). We estimated the binding potentials of five subjects with DMXB-A inhibition in the baseline and at inhibition, using the values of $V_{T(b)}$ and $V_{ND(b)}$ in the baseline condition, and the values of $V_{T(i)}$ and $V_{ND(i)}$ at inhibition obtained by means of equation (2), in the unblocked and DMXB-A inhibited states, with the equations,

$$BP_{\mathrm{ND(b)}} = \frac{V_{\mathrm{T(b)}}}{V_{\mathrm{ND(b)}}} - 1 \quad \text{and} \quad BP_{\mathrm{ND(i)}} = \frac{V_{\mathrm{T(i)}}}{V_{\mathrm{ND(i)}}} - 1 \qquad (3)$$

where the $BP_{\mathrm{ND\,(b)}}$ and $BP_{\mathrm{ND(i)}}$ terms symbolize the binding potentials at baseline and inhibition, respectively.

The binding potentials (BP_{ND}) and inhibitor concentrations (Ci) yielded the B_{max} and K_I (IC_{50}) estimates of the receptor and inhibitor, respectively. We completed receptor density (B_{max}) and affinity of the competitor (IC_{50}, K_I) calculation of α7-nAChR in five subjects by means of DMXB-A inhibition, using the values of BP_{ND} of baseline and inhibition that led to the novel (never previously published) in vivo estimate of the magnitude of the receptor density (B_{max}) and affinity (K_I) of nAChR in humans, using the equation,

$$BP_{\mathrm{ND}} = \frac{B_{\mathrm{max}}}{K_{\mathrm{d}}\left(1 + \frac{[\mathrm{DMXB\text{-}A}]}{K_{\mathrm{I}}}\right)} \qquad (4)$$

where the receptor density is determined relative to the affinity of the radioligand to the receptor, K_d, with known values of the inhibitor concentration [DMXB-A] and the receptor's affinity for inhibitor, K_I. For this calculation we used a calculated value of ASEM K_d of 0.35 nM (established from prior measure of K_I of 0.4 nM for [^{123}I] bungarotoxin).

Schizophrenia

Six patients with schizophrenia were compared to a subset of 15 healthy volunteers matched for age, in this subset with mean age of healthy volunteers 23 ± 4 (SD) years, range 18-30; and with patients with schizophrenia mean age 24 ± 4 (SD) years, range 20-31 years in cingulate, frontal cortex and hippocampus.

Results

Regional Volumes of Distribution

Regional estimates of volumes of distribution (V_T) in selected regions are shown in Figure 1A. We tested the test-retest variability of the V_T estimates in eight healthy subjects, six males (average age 41) and two females (average age 24). Across all cortical and subcortical VOIs, the average test-retest variability was 7.8% ± 0.6% (SD, see Figure 1B), ranging from 6.5% to 8.9%. (repeatability of > 90% .)

Receptor Kinetics

The reanalysis of inhibition of [^{18}F]ASEM binding in baboon (Horti et al., 2014) yielded the V_T of non-displaceable tracer accumulation at baseline ($V_{ND(b)}$), In the baboon, the V_T of [^{18}F]ASEM declined markedly in response to blocking with the high affinity inhibitor SSR180711. The reference volume V_{ND} assessed by means of the standard Inhibition Plot (IP) is presented in Figure 2, with the estimate of $V_{ND\ (b)}$ of 5.4 ml/cm^3 at the lower dose of the SR180711. We note that the magnitude of V_{ND} is a property of the tracer [^{18}F]ASEM that we assume to be representative of mammalian brains in general.

We used the value of V_{ND} of 5.4 ml/cm^3 as the value of $V_{ND\ (b)}$ in the Extended Inhibition Plot (EIP), required when V_T values failed to yield evidence of inhibition of radioligand binding by DMXB-A in human brain. In five subjects, the value of $V_{ND(b)}$ yielded estimates of saturation (s) and inhibition reference volume ($V_{ND(i)}$), as shown in Figure 2 of the individual estimates of s as function of the concentration of DMXB-A in arterial plasma, confirming the dose-dependent inhibition exerted by DMXB-A. Estimates of regional binding potentials (BP_{ND}) declined significantly in 6 of the 21 representative regions after blocking with DMXB-A, as shown in Figure 3. The average values for all 21 regions of receptor density (B_{max}) and average values of the receptor's affinity (K_I) to DMXB-A for ranged from 0.67-0.82 nM for B_{max} and from 170 to 385 nM for K_I, as presented in Figure 4. Regarding the choice of the $V_{ND\ (b)}$ the standard error of the $V_{ND\ (b)}$ estimate in baboon of 2.7 ml/cm^3 corresponded to ranges of human B_{max} estimates of 0.4-1.9 nM and DMXB-A KI estimates of 138-363 nM.

Menstrual Cycle

The menstrual cycle phase (luteal vs. follicular) was determined for the eight healthy control females. Estimates of V_T did not differ significantly in relation to cycle phase. The lower ages of women volunteers precluded analysis of different changes of V_T with age in men and women.

Schizophrenia

In the three preselected regions (cingulate and frontal cortices, hippocampus) examined for group differences between patients and the age-matched control subjects, the median V_T values were lower in patients than in age-matched healthy volunteers (Figure 5). Potential outliers, one a control subject and one a patient, were identified (outlier points marked in boxplots of Figure 5). Using the Mann-Whitney U-test, we tested for significant differences of median V_T values between control subjects and patients, before and after excluding outliers. The results, with corrections for multiple comparisons, are given in Table 2. In the cingulate cortex and hippocampus, the difference of V_T

values was significant after exclusion of outliers and correction for multiple comparisons (P = 0.02 in both regions).

The correlation of V_T with BPRS did not reach statistical significance although there were positive trends for 5 subjects in the cingulate and frontal cortex after outlier analyses (see Supplementary Figure C for details).

Antipsychotic medication

The biodistribution in mice revealed no significant effects on [^{18}F]ASEM binding of aripriprizole, risperidone, or olanzapine (see Supplemental materials). As described in methods tne patient with schizophrenia chronically treated with risperidone had repeated PET after a 3-week drug-free period, imposed for clinical reasons. The V_T estimates did not differ by more than 7% (i.e., within the test-retest variability of control subjects (Figure 1B)) in any brain region for the on- and off–risperidone comparison. (Supplementary Figure C, points labelled "on" and "off").

Discussion

Subjects

We extended the first-in-human report of (Wong et al., 2014) from five to 21 healthy subjects (eight test-retest sessions, five sessions with inhibition by DMXB-A of [^{18}F]ASEM binding, and six baseline sessions) and added a preliminary study of six patients with schizophrenia, with one patient receiving test-retest PET in the absence and presence of chronic risperidone medication.

The results demonstrate excellent test-retest repeatability of [^{18}F]ASEM PET of more than 90%. In the population of 21 healthy non-smoking volunteers, when we plotted tracer distribution volume V_T against age we observed an increase with of V_T with age. While our smaller sample and lack of a wide age distribution limited our ability to test this relationship formally with regression analysis, the trends in our data match the findings from a larger age range in another set of subjects (Coughlin et al., 2017; which had only 2 subjects in common which we provided to the Coughlin paper previously). These V_T vs age preliminary findings are shown in Supplementary Figure D.

We were unable to determine sex differences because of the different age ranges. Of the eight women, none showed a specific effect of menstrual cycle on estimates of V_T.

Receptor binding potentials

Estimates of receptor density (B_{max}) are based on determination of binding potentials BP_{ND} (Gjedde et al., 2005). Importantly, for the first time, we present evidence that competitor occupancy, apparent inhibitor affinity (K_I), and receptor density (B_{max}) of human α7-nAChR can be measured, based on the assumptions presented. We determined regional estimates of [^{18}F] ASEM binding as the first step towards complete receptor quantification. In addition to regional values of V_T, the receptor quantification required knowledge of the magnitude of V_T of the tracer in a region of brain tissue with no specific binding. Previously, no such reference volume has been identified for this tracer with prevalent binding in cerebral cortex. As the first PET study with blockade of α7-nAChR in human brain in vivo, this study took advantage of the original development of the well-documented partial agonist DMXB-A at the University of Florida (Kem, 2000; Kem et al., 2004) and the subsequent successful testing in patients with schizophrenia at the University of Colorado (Olincy et al., 2006; Freedman, 2014).

Receptor occupancy

Recent studies of mouse and baboon brains revealed significant blockade of the α7-nAChR by the high affinity partial α7-nAChR agonists SSR180711 and DMXB-A in vivo (Horti et al., 2014a; Wong et al., 2014), but effective inhibition or competition has not yet been confirmed in humans. As a candidate drug, DMXB-A was tested in clinical trials of patients with schizophrenia, Alzheimer's disease, or ADHD (Freedman et al., 2008; Freedman, 2014), and the drug was used here to test target engagement/occupancy in vivo at the α7-nAChR and to demonstrate specificity of [^{18}F]ASEM binding to these receptors.

Previously, we demonstrated dose-dependent tracer inhibition in rodents by DMXB-A with cerebellum as reference region (appropriate in rodents but not human brain) (Wong et al., 2014). Similarly, in the present study, blockade with the highest dose of DMXB-A allowed in humans (150

mg orally) exhibited competition with binding of [^{18}F]ASEM . The occupancy of receptors by DMXB-A displayed a relatively monotonic relationship with plasma levels of DMXB-A.

We used the Extended Inhibition Plot (EIP) under the assumption that the apparently absent inhibition of receptor binding would be due to factors such as change of free fractions of the radioligand in circulation or brain tissue or both, with the consequence that the value of V_{ND} would differ between the baseline ($V_{ND\,(b)}$) and inhibited ($V_{ND\,(a)}$) states, as reported by Phan et al. (2017). Using EIP and the value of $V_{ND(b)}$ of 5.4 ml/cm^3 obtained from moderate blockade of the α7-nAChR in baboon brain, reported by Horti et al. (2014) as a simple reduction in slope and reanalyzed by the standard Inhibition Plot (IP) here, we obtained DMXB-A occupancies in the human subjects in the range of 17-49%. Future studies with new α7-nAChR drugs will further test the occupancy and the accuracy of the resulting estimates of receptor density and affinity in human brain in vivo.

With the assumptions and translation from autopsy protein and wet tissue based receptor densities (B_{max}) of α7-nAChR, we find remarkable agreement among the B_{max} estimates that we regard as another innovative aspect of the present study. As 150 mg is the highest single oral dose allowed under the DXMB-A IND based on historical information, we elected not to test lower doses, because of the modest occupancy, compared to occupancy of drugs such as antipsychotics, and more recently glycine transporter (GlyT1) ligands ((Martin-Facklam et al., 2013; Wong et al., 2013), the dose dependent occupancy with DMXB-A is evidence of specificity of the radiotracer [^{18}F]ASEM in human brain. The occupancy is further evidence of the potential usefulness of [^{18}F]ASEM for therapeutic occupancy trials, as these are somewhat complicated due to the inverted-U shaped dose effect of α7-nAChR partial agonists (Young and Geyer, 2013).

The α7-nAChR receptor has five binding sites among the five α7 subunits and is maximally activated when at least two binding sites are occupied by an agonist. At higher doses, agonists bind at up to all five binding sites and progressively desensitize the α7. Moreover, α7 partial agonist drugs such as DMXB-A and others produce their clinical effects at lower concentrations than would be expected from *in vitro* functional experiments where peak currents are recorded (Prickaerts et al., 2012; Papke, 2014; Preskorn et al., 2014). The co-agonistic mechanism of *in vivo* action of α7 partial agonist suggests that DMXB-A, at the clinically effective dose, binds at one of five binding sites of α7, while brisk activation of the receptor will, however, occur upon exposure to endogenous ACh. Thus, *in vivo*, a single molecule of DMXB-A plus one molecule of ACh are sufficient to trigger the opening of the α7-nAChR channel (Williams et al., 2011; Prickaerts et al., 2012; Papke, 2014; Preskorn et al., 2014). Therefore, in the PET occupancy studies with the DMXB-A-treated humans, the binding of [^{18}F]ASEM is expected to be inhibited by as little as 20-40% (1/5th - 2/5th) instead of 100%. This co-agonistic mechanism agrees reasonably with our PET [^{18}F]ASEM inhibition by DMXB-A in humans at 17-49% with a maximum clinical dose of DMXB-A (150 mg). Full blocking of [^{18}F]ASEM with α7 agonists occurs at higher doses, as observed in mice with 20 mg/kg DMXB-A (Horti et al., 2014a; Wong et al., 2014) and in baboons administered 5 mg/kg of the more highly potent SSR180711 that is unavailable in the US (Horti et al., 2014).

Receptor Density and Tracer Affinity

The use of the EIP with the DMXB-A inhibition and the use of the estimate of V_{ND} from baboon brain (Horti *et al,* 2014) yielded the binding potentials necessary to estimate in vivo the average values across all binding regions of B_{max} (0.67-0.82 nM)) and K_I (range 170-385) in human brain. While the value of V_{ND} in humans currently is unknown, the baboon value of 5.4 ml/cm^3 estimated here with SEM of 2.7 ml/cm^3 corresponded to ranges of B_{max} estimates of 0.75 (range 0.38-1.83) nM and DMXB-A K_I estimates of 138-363 nM. These values agree favorably with estimates postmortem of 0.28 nM B_{max} for human cerebral cortex with α-[^{125}I]bungarotoxin (Davies and Feisullin, 1981) and cortical B_{max} values of 0.7 nM in patients with schizophrenia compared to 1.5 nM in healthy control subjects (Marutle et al., 2001), assuming 10% mg protein converted to wet weight.

Schizophrenia

Preliminary analysis of six patients with schizophrenia tested abnormalities of α7-nAChR. The finding of significant reduction of regional distribution in five of six subjects in two of three regions after outlier exclusion of a single subject agreed with previous findings post-mortem.

Limitations

Antipsychotic medication

Neuroreceptor studies of patients with schizophrenia in the drug free or naïve state is increasingly logistically challenging, although such studies have been completed in limited populations (Farde et al., 1986; Wong et al., 1986). In the present limited population, patients with schizophrenia were tested while on stable medication for more than three weeks with antipsychotics that are held to have only negligible effect on binding to α7 nAchR, and to be non-exclusionary in therapeutic studies of partial agonists such as DXMB-A, e.g., clozapine. Several precautions were taken to reduce the possibility of confounding antipsychotic action in the quantification of binding to α7nAchR. First, the majority of the patients were treated with risperidone and haloperidol, which unlike clozapine fail to normalize the P50 abnormality (Adler et al., 1998). Second, a rodent biodistribution study found no significant effects on [^{18}F]ASEM binding. Finally, although only one subject was studied off medications, the repeated PET test on- and off- chronic risperidone was suggestive of the conclusion that this commonly used antipsychotic is unlikely to confound the estimates of the V_T values for $_{\alpha 7}$ nAChR.

Smoking

Despite the relatively high prevalence of smoking in patients with schizophrenia, only one of the subjects with schizophrenia smoked (20 cigarettes a day). The V_T values did not differ significantly for the smoking subject compared to two other patients with schizophrenia with a low value of V_T. All told, all 21 control subjects and 5 of the 6 patients with schizophrenia were non-smokers. Thus, while future studies will require careful matching in larger populations, given that 5 out of the 6 patients with schizophrenia were non-smokers, this is not likely to be a confound. Furthermore, on the day of PET, all control and patients with schizophrenia had CO less than 4 PPM indicating they successfully were abstinent (regardless of their self-report) and likely longer than 12 hrs reducing the acute effects of nicotine, if any, on the PET measure of the tracer volume of distribution (V_T).

Age and sex differences

In the group of 21 subjects in the age range of 18 to 50 years, males and females were not distributed uniformly, ruling out formal determination of sex differences as functions of normal aging. Also, the small number of five subjects with DXMB-A occupancy nonetheless yielded a reasonable range of DXMB-A human plasma concentrations, presumably due to individual variability in oral absorption and metabolism of the inhibitor.

Schziophrenia

Finally, the small number of patients with schizophrenia is a limitation. While we have completed extensive neuropsychology testing on these six subjects, the results are too preliminary to sufficiently report here in the pilot study. Nevertheless five of the six showed reduced estimates of V_T in two of the three regions compared to age matched controls thus encouraging expansion of the number of patients studied with this novel α7nAchR radiotracer.

Conclusions

Here, we confirmed the test-retest reliability of tracer binding in healthy human brains, and we demonstrated for the first time specificity of competition from the partial agonist DMXB-A in normal healthy volunteers, as previously reported in preclinical imaging studies. The novel first time presented in vivo B_{max} measures agreed favorably with published human postmortem values. The effects of antipsychotics in our schizophrenia volunteers may not be a major confound based on our preliminary mice and literature and one subject on and off risperidone. The preliminary findings in patients with schizophrenia are intriguingly consistent with previous reports of human brains post-mortem, but clearly larger samples with a spectrum of clinical severity and comparisons with full cognitive and neuropsychological tests are needed.

Funding and Disclosure

The authors declare no conflicts of interest, including relevant financial interests, activities, relationships, and affiliations. All work under PHS NIH grant 2 R01 MH107197

Acknowledgements

Robert F Dannals and Radiochemistry staff, Johns Hopkins PET Center staff , David Schretlen, PhD and J Coughlin , MD for scientific discussions and the High Resolution Brain Imaging Section faculty, staff and fellows. Thanks to Gayane Yenokyan, MD, PhD, Director, Biostatistics Consulting Center, Johns Hopkins School of Public Health for guidance and assistance on statistical analyses.

References

Adler LE, Olincy A, Waldo M, Harris JG, Griffith J, Stevens K, Flach K, Nagamoto H, Bickford P, Leonard S, Freedman R (1998) Schizophrenia, sensory gating, and nicotinic receptors. Schizophrenia bulletin 24:189-202.

AhnAllen CG (2012) The role of the alpha7 nicotinic receptor in cognitive processing of persons with schizophrenia. Curr Opin Psychiatry 25:103-108.

Albuquerque EX, Pereira EF, Alkondon M, Rogers SW (2009) Mammalian nicotinic acetylcholine receptors: from structure to function. Physiol Rev 89:73-120.

Anderson DJ, Arneric SP (1994) Nicotinic receptor binding of 3H]cytisine, 3H]nicotine and 3H]methylcarbamylcholine in rat brain. Eur J Pharmacol 253:261-267.

Ashburner J, Friston KJ (2003) Rigid body registration. In: Human Brain Function, 2nd Edition (Frackowiak RSJ, Friston KJ, Frith C, Dolan R, Friston KJ, Price CJ, Zeki S, Ashburner J, Penny WD, eds): Academic Press.

Beinat C, Banister SD, Herrera M, Kassiou M (2016) The Recent Development of alpha7 Nicotinic Acetylcholine Receptor (nAChR) Ligands as Therapeutic Candidates for the Treatment of Central Nervous System (CNS) Diseases. Curr Pharm Des 22:2134-2151.

Beinat C, Banister SD, Herrera M, Law V, Kassiou M (2015) The therapeutic potential of alpha7 nicotinic acetylcholine receptor (alpha7 nAChR) agonists for the treatment of the cognitive deficits associated with schizophrenia. CNS Drugs 29:529-542.

Coughlin JM et al. (2017) The distribution of the alpha7 nicotinic acetylcholine receptor in healthy aging: An in vivo positron emission tomography study with [(18)F]ASEM. NeuroImage 165:118-124.

Court J, Spurden D, Lloyd S, McKeith I, Ballard C, Cairns N, Kerwin R, Perry R, Perry E (1999) Neuronal nicotinic receptors in dementia with Lewy bodies and schizophrenia: alpha-bungarotoxin and nicotine binding in the thalamus. J Neurochem 73:1590-1597.

D'Hoedt D, Bertrand D (2009) Nicotinic acetylcholine receptors: an overview on drug discovery. Expert Opin Ther Targets 13:395-411.

Davies AR, Hardick DJ, Blagbrough IS, Potter BV, Wolstenholme AJ, Wonnacott S (1999) Characterisation of the binding of 3H]methyllycaconitine: a new radioligand for labelling alpha 7-type neuronal nicotinic acetylcholine receptors. Neuropharmacology 38:679-690.

Davies P, Feisullin S (1981) Postmortem stability of alpha-bungarotoxin binding sites in mouse and human brain. Brain research 216:449-454.

Dawe GS, Nagarajah R, Albert R, Casey DE, Gross KW, Ratty AK (2010) Antipsychotic drugs dose-dependently suppress the spontaneous hyperactivity of the chakragati mouse. Neuroscience 171:162-172.

Ettrup A, Mikkelsen JD, Lehel S, Madsen J, Nielsen EO, Palner M, Timmermann DB, Peters D, Knudsen GM (2011) 11C-NS14492 as a novel PET radioligand for imaging cerebral alpha7 nicotinic acetylcholine receptors: in vivo evaluation and drug occupancy measurements. J Nucl Med 52:1449-1456.

Farde L, Hall H, Ehrin E, Sedvall G (1986) Quantitative analysis of D2 dopamine receptor binding in the living human brain by PET. Science 231:258-261.

Fischl B, van der Kouwe A, Destrieux C, Halgren E, Segonne F, Salat DH, Busa E, Seidman LJ, Goldstein J, Kennedy D, Caviness V, Makris N, Rosen B, Dale AM (2004) Automatically parcellating the human cerebral cortex. Cerebral cortex (New York, NY : 1991) 14:11-22.

Freedman R (2014) Alpha7-Nicotinic Acetylcholine Receptor Agonists for Cognitive Enhancement in Schizophrenia. Annual Review of Medicine 65:245-261.

Freedman R, Hall M, Adler LE, Leonard S (1995) Evidence in postmortem brain tissue for decreased numbers of hippocampal nicotinic receptors in schizophrenia. Biological Psychiatry 38:22-33.

Freedman R, Olincy A, Buchanan RW, Harris JG, Gold JM, Johnson L, Allensworth D, Guzman-Bonilla A, Clement B, Ball MP, Kutnick J, Pender V, Martin LF, Stevens KE, Wagner BD, Zerbe GO, Soti F, Kem WR (2008) Initial phase 2 trial of a nicotinic agonist in schizophrenia. The American Journal of Psychiatry 165:1040-1047.

Gao Y, Kellar KJ, Yasuda RP, Tran T, Xiao Y, Dannals RF, Horti AG (2013) Derivatives of Dibenzothiophene for Positron Emission Tomography Imaging of alpha7-Nicotinic Acetylcholine Receptors. J Med Chem 56:7574-7589.

Geerts H (2012) alpha7 Nicotinic receptor modulators for cognitive deficits in schizophrenia and Alzheimer's disease. Expert Opin Investig Drugs 21:59-65.

Gjedde A, Wong DF (2000) Receptor occupancy in absence of reference region. Neuroimage 11:S48.

Gjedde A, Wong DF, Rosa-Neto P, Cumming P (2005) Mapping neuroreceptors at work: on the definition and interpretation of binding potentials after 20 years of progress. International review of neurobiology 63:1-20.

Gotti C, Clementi F (2004) Neuronal nicotinic receptors: from structure to pathology. Prog Neurobiol 74:363-396.

Guan ZZ, Zhang X, Blennow K, Nordberg A (1999) Decreased protein level of nicotinic receptor alpha7 subunit in the frontal cortex from schizophrenic brain. Neuroreport 10:1779-1782.

Hillmer AT, Li S, Zheng MQ, Scheunemann M, Lin SF, Nabulsi N, Holden D, Pracitto R, Labaree D, Ropchan J, Teodoro R, Deuther-Conrad W, Esterlis I, Cosgrove KP, Brust P, Carson RE, Huang Y (2017) PET imaging of alpha7 nicotinic acetylcholine receptors: a comparative study of [18F]ASEM and [18F]DBT-10 in nonhuman primates, and further evaluation of [18F]ASEM in humans. Eur J Nucl Med Mol Imaging.

Hoffmeister PG, Donat CK, Schuhmann MU, Voigt C, Walter B, Nieber K, Meixensberger J, Bauer R, Brust P (2011) Traumatic brain injury elicits similar alterations in alpha7 nicotinic receptor density in two different experimental models. Neuromolecular Med 13:44-53.

Horti AG (2015) Development of [F]ASEM, a specific radiotracer for quantification of the alpha7-nAChR with positron-emission tomography. Biochem Pharmacol..

Horti AG, Gao Y, Kuwabara H, Wang Y, Abazyan S, Yasuda RP, Tran T, Xiao Y, Sahibzada N, Holt DP, Kellar KJ, Pletnikov MV, Pomper MG, Wong DF, Dannals RF (2014) 18F-ASEM, a radiolabeled antagonist for imaging the alpha7-nicotinic acetylcholine receptor with PET. J Nucl Med 55:672-677.

Ishikawa M, Hashimoto K (2011) alpha7 nicotinic acetylcholine receptor as a potential therapeutic target for schizophrenia. Curr Pharm Des 17:121-129.

Jenkinson M, Beckmann CF, Behrens TE, Woolrich MW, Smith SM (2012) FSL. Neuroimage 62:782-790.

Kem WR (2000) The brain alpha7 nicotinic receptor may be an important therapeutic target for the treatment of Alzheimer's disease: studies with DMXBA (GTS-21). Behavioural brain research 113:169-181.

Kem WR, Mahnir VM, Prokai L, Papke RL, Cao X, LeFrancois S, Wildeboer K, Prokai-Tatrai K, Porter-Papke J, Soti F (2004) Hydroxy metabolites of the Alzheimer's drug candidate 3-[(2,4-dimethoxy)benzylidene]-anabaseine dihydrochloride (GTS-21): their molecular properties, interactions with brain nicotinic receptors, and brain penetration. Molecular pharmacology 65:56-67.

Lewis AS, van Schalkwyk GI, Bloch MH (2017) Alpha-7 nicotinic agonists for cognitive deficits in neuropsychiatric disorders: A translational meta-analysis of rodent and human studies. Prog Neuropsychopharmacol Biol Psychiatry 75:45-53.

Lukas RJ, Changeux JP, Le Novere N, Albuquerque EX, Balfour DJ, Berg DK, Bertrand D, Chiappinelli VA, Clarke PB, Collins AC, Dani JA, Grady SR, Kellar KJ, Lindstrom JM, Marks MJ, Quik M, Taylor PW, Wonnacott S (1999) International Union of Pharmacology. XX. Current status of the nomenclature for nicotinic acetylcholine receptors and their subunits. Pharmacol Rev 51:397-401.

Magnussen JH, Ettrup A, Donat CK, Peters D, Pedersen MH, Knudsen GM, Mikkelsen JD (2015) Radiosynthesis and in vitro validation of H-NS14492 as a novel high affinity alpha7 nicotinic receptor radioligand. Eur J Pharmacol 762:35-41.

Marrero MB, Bencherif M, Lippiello PM, Lucas R (2011) Application of alpha7 nicotinic acetylcholine receptor agonists in inflammatory diseases: an overview. Pharm Res 28:413-416.

Martin-Facklam M, Pizzagalli F, Zhou Y, Ostrowitzki S, Raymont V, Brašić JR, Parkar N, Umbricht D, Dannals RF, Goldwater R, Wong DF (2013) Glycine transporter type 1 occupancy by bitopertin: a positron emission tomography study in healthy volunteers. Neuropsychopharmacology : official publication of the American College of Neuropsychopharmacology 38:504.

Marutle A, Zhang X, Court J, Piggott M, Johnson M, Perry R, Perry E, Nordberg A (2001) Laminar distribution of nicotinic receptor subtypes in cortical regions in schizophrenia. J Chem Neuroanat 22:115-126.

McOmish CE, Lira A, Hanks JB, Gingrich JA (2012) Clozapine-induced locomotor suppression is mediated by 5-HT2A receptors in the forebrain. Neuropsychopharmacology : official publication of the American College of Neuropsychopharmacology 37:2747-2755.

Ning H, Cao D, Wang H, Kang B, Xie S, Meng Y (2017) Effects of haloperidol, olanzapine, ziprasidone, and PHA-543613 on spatial learning and memory in the Morris water maze test in naive and MK-801-treated mice. Brain and behavior 7:e00764.

Olincy A, Harris JG, Johnson LL, Pender V, Kongs S, Allensworth D, Ellis J, Zerbe GO, Leonard S, Stevens KE, Stevens JO, Martin L, Adler LE, Soti F, Kem WR, Freedman R (2006) Proof-of-concept trial of an alpha7 nicotinic agonist in schizophrenia. Archives of General Psychiatry 63:630-638.

Papke RL (2014) Merging old and new perspectives on nicotinic acetylcholine receptors. Biochemical pharmacology 89:1-11.

Parri HR, Hernandez CM, Dineley KT (2011) Research update: Alpha7 nicotinic acetylcholine receptor mechanisms in Alzheimer's disease. Biochem Pharmacol 82:931-942.

Patenaude B, Smith SM, Kennedy DN, Jenkinson M (2011) A Bayesian model of shape and appearance for subcortical brain segmentation. NeuroImage 56:907-922.

Phan J, Landua A, Jakobsen S, Gjedde A (2017) Radioligand binding analysis of α2 adrenoceptors with [11C]yohimbine in brain in vivo: Extended inhibition plot correction for plasma protein binding. Scientific Reports. 2017;7(1):15979.

Philip NS, Carpenter LL, Tyrka AR, Price LH (2010) Nicotinic acetylcholine receptors and depression: a review of the preclinical and clinical literature. Psychopharmacology (Berl) 212:1-12.

Potasiewicz A, Holuj M, Kos T, Popik P, Arias HR, Nikiforuk A (2017) 3-Furan-2-yl-N-p-tolyl-acrylamide, a positive allosteric modulator of the alpha7 nicotinic receptor, reverses schizophrenia-like cognitive and social deficits in rats. Neuropharmacology 113:188-197.

Preskorn SH, Gawryl M, Dgetluck N, Palfreyman M, Bauer LO, Hilt DC (2014) Normalizing effects of EVP-6124, an alpha-7 nicotinic partial agonist, on event-related potentials and cognition: a proof of concept, randomized trial in patients with schizophrenia. Journal of psychiatric practice 20:12-24.

Prickaerts J, van Goethem NP, Chesworth R, Shapiro G, Boess FG, Methfessel C, Reneerkens OA, Flood DG, Hilt D, Gawryl M, Bertrand S, Bertrand D, Konig G (2012) EVP-6124, a novel and selective alpha7 nicotinic acetylcholine receptor partial agonist, improves memory performance by potentiating the acetylcholine response of alpha7 nicotinic acetylcholine receptors. Neuropharmacology 62:1099-1110.

Reagan-Shaw S, Nihal M, Ahmad N (2008) Dose translation from animal to human studies revisited. FASEB journal : official publication of the Federation of American Societies for Experimental Biology 22:659-661.

Thomsen MS, Hansen HH, Timmerman DB, Mikkelsen JD (2010) Cognitive improvement by activation of alpha7 nicotinic acetylcholine receptors: from animal models to human pathophysiology. Curr Pharm Des 16:323-343.

Toyohara J, Sakata M, Wu J, Ishikawa M, Oda K, Ishii K, Iyo M, Hashimoto K, Ishiwata K (2009) Preclinical and the first clinical studies on [C-11]CHIBA-1001 for mapping alpha 7 nicotinic receptors by positron emission tomography. Ann Nucl Med 23:301-309.

Verbois SL, Scheff SW, Pauly JR (2002) Time-dependent changes in rat brain cholinergic receptor expression after experimental brain injury. J Neurotrauma 19:1569-1585.

Verbois SL, Sullivan PG, Scheff SW, Pauly JR (2000) Traumatic brain injury reduces hippocampal alpha7 nicotinic cholinergic receptor binding. J Neurotrauma 17:1001-1011.

Wallace TL, Bertrand D (2013) Alpha7 neuronal nicotinic receptors as a drug target in schizophrenia. Expert opinion on therapeutic targets 17:139-155.

Wallace TL, Bertrand D (2015) Neuronal alpha7 Nicotinic Receptors as a Target for the Treatment of Schizophrenia. Int Rev Neurobiol 124:79-111.

Wallace TL, Callahan PM, Tehim A, Bertrand D, Tombaugh G, Wang S, Xie W, Rowe WB, Ong V, Graham E, Terry Jr AV, Rodefer JS, Herbert B, Murray M, Porter R, Santarelli L, Lowe DA

(2011) RG3487, a novel nicotinic alpha7 receptor partial agonist, improves cognition and sensorimotor gating in rodents. J Pharmacol Exp Ther 336:242-253.

Williams DK, Wang J, Papke RL (2011) Investigation of the molecular mechanism of the alpha7 nicotinic acetylcholine receptor positive allosteric modulator PNU-120596 provides evidence for two distinct desensitized states. Molecular pharmacology 80:1013-1032.

Wong DF, Ostrowitzki S, Zhou Y, Raymont V, Hofmann C, Borroni E, Kumar A, Parkar N, Brasic JR, Hilton J, Dannals RF, Martin-Facklam M (2013) Characterization of [11C]RO5013853, a novel PET tracer for the glycine transporter type 1 (GlyT1) in humans. Neuroimage 75:282-290.

Wong DF, Kuwabara H, Roberts J, Brasic J, Mishra C, Kitzmiller K, McDonald M, Gapasin L, Nandi A, Wand G, Gjedde A, Horti A (2017) [F-18] ASEM PET imaging of the alpha 7 nicotinic cholinergic receptor: test retest and sex differences. J Cereb Blood Flow Metab 37:79-79.

Wong DF, Kuwabara H, Pomper M, Holt DP, Brasic JR, George N, Frolov B, Willis W, Gao Y, Valentine H, Nandi A, Gapasin L, Dannals RF, Horti AG (2014) Human Brain Imaging of Alpha-7 nAChR with 18F]ASEM: a New PET Radiotracer for Neuropsychiatry and Determination of Drug Occupancy. Molecular Imaging and Biology 16:730-738.

Wong DF, Wagner HN, Jr., Tune LE, Dannals RF, Pearlson GD, Links JM, Tamminga CA, Broussolle EP, Ravert HT, Wilson AA, Toung JK, Malat J, Williams JA, O'Tuama LA, Snyder SH, Kuhar MJ, Gjedde A (1986) Positron emission tomography reveals elevated D2 dopamine receptors in drug-naive schizophrenics. Science 234:1558-1563.

Woodruff-Pak DS, Gould TJ (2002) Neuronal nicotinic acetylcholine receptors: involvement in Alzheimer's disease and schizophrenia. Behav Cogn Neurosci Rev 1:5-20.

Young JW, Geyer MA (2013) Evaluating the role of the alpha-7 nicotinic acetylcholine receptor in the pathophysiology and treatment of schizophrenia. Biochem Pharmacol 86:1122-1132.

Table 1A: Group Demographics

DIAGNOSIS	CONDITION	N	MALES	FEMALES	AGE (*M/SD*)	AGE (*RANGE*)
HEALTHY CONTROLS*	Baseline	21	13	8	32.0 (12.4)	18-52
	Retest	8	6	2	37.8 (11.7)	20-52
	Blocking	5	3	2	22.1 (4.5)	18-28
PATIENTS WITH SCHIZOPHRENIA	Baseline	6	6	0	24.8 (3.9)	20-31

*No Healthy controls reported current or past smoking hsitory

Table 1B: Patients with Schizophrenia

Subject ID	**Age**	**Sex**	**Race**	**Ethnicity**	**BPRS – Negative (*M*)**	**BPRS – Positive (*M*)**	**Smoker**	**Cig/day**	**Medications**
01	27	M	AA	NH	2.25	1.25	No	N/A	Aripiprazole
02	31	M	W	NH	3	1	Yes	20	Haloperidol, Benztropine, Sertraline
03	22	M	AA	NH	2.75	2.25	No	N/A	Risperidone
04	25	M	AA	NH	2.75	1.75	No	N/A	Quetiapine, Haloperidol, Benztropine
05	20	M	AA	NH	1.5	1.5	No	N/A	Escitalopram, Benztropine, Aripiprazole, Clonezapam
06 – Scan 1	24	M	W	NH	2.75	3.25	No	N/A	Risperidone, Lorazepam
06- Scan 2	24	M	W	NH	1.0	1.0	No	N/A	Lorazepam

Table 2: Corrected and uncorrected P values from V_T in controls vs. patients.

Results (uncorrected P values and corrected by different methods) of Mann-Whitney tests for V_T in Healthy Controls vs. Patients with Schizophrenia. Adjusted p values were obtained by the STATA package *qqvalue* using three different methods of adjustment (Newsom, 2010; specific methods are Horcberg, 1998, standard Bonferroni correction and Simes, 1986).

Region	Uncorrected P value	Adjusted (Horchberg)	Adjusted (Bonferroni)	Adjusted (Simes)
		All Data		
Cg	0.056	0.159	0.167	0.118
Fr	0.171	0.172	0.515	0.172
Hp	0.079	0.159	0.238	0.119
		With Outliers removed		
Cg	0.009	0.028	0.028	0.025
Fr	0.058	0.058	0.173	0.058
Hp	0.017	0.033	0.05	0.025

Figure Legends

Fig. 1: Estimates of V_T and Test-Retest Variability for V_T.

1A: Regional estimates of V_T, for all healthy control subjects (n=21). **1B:** Test-Retest variability of V_T in eight healthy controls. For both panels, bars show mean +/- SD. **Regional Abbreviations:** Am: amygdala; CN: caudate nucleus; Cb: cerebellum; Cg: cingulate; Fr: frontal lobe; Fs: fusiform gyrus; GP: globus pallidus; Hp: hippocampus; In: insula; LG: lingular gyrus; Oc occipital lobe; pC: paracentral; PH: Parahippocampus; Pa: parietal lobe; PS: postcentral gyrus; Pc: precentral gyrus; Pr: precuneus; Pu: putamen; Tp: temporal lobe; Th: thalamus; vS: ventral striatum.

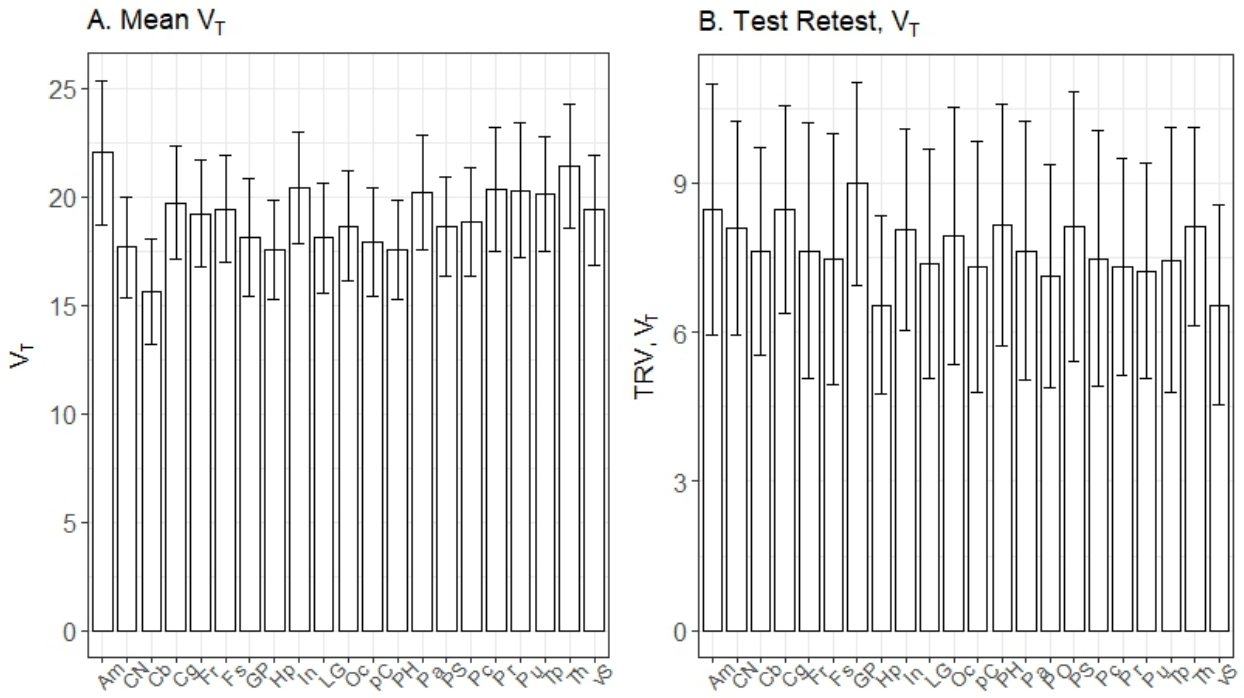

Fig. 2. Dose-Dependent Inhibition with DMXB-A level

The saturation, *s*, reflects the fraction of receptor occupied by the blocking agent, DMXB-A. Each point on the curve represents individual measurements of the plasma level of DMXB-A, determined by mass spectroscopy, and the fraction of receptors occupied by DMXB-A, estimated by the Extended Inhibition Plot. The horizontal error bars represent the S.E.M from three measurements, and the vertical error bars reflect the S.E.M from the linear analysis of the Extended Inhibition plot. These data were fit to the Michaelis-Menten equation, with O_{max} assigned to a value of 1; (i.e, 100% occupancy, or a saturation fraction, $s = 1$). This is typical for receptor occupancy studies with PET. However, further studies at higher plasma concentrations may indicate a lower maximal occupancy, due to the unique nature of the α7 subunit, as stated in the Discussion.

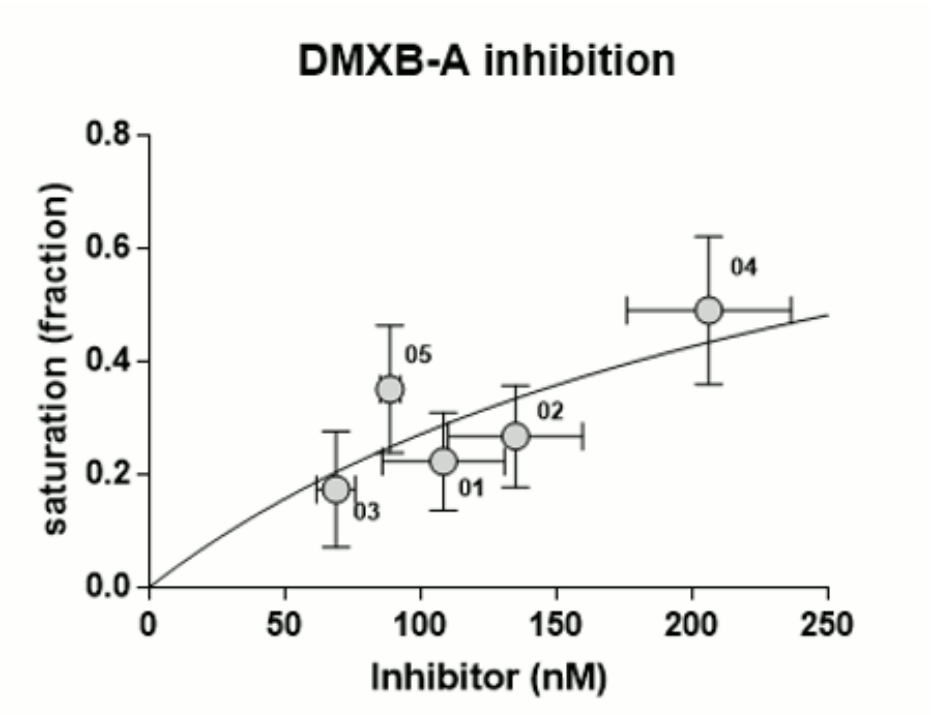

Fig. 3. Regional Binding Potentials (BP_{ND})

The analysis using the Extended Inhibition plot revealed that the binding potential, BP_{ND}, decreased significantly in response to competition with DMXB-A by 31% in average when compared to baseline. Each line on the graphs of six representative regions of the original 21 regions displays the estimates of BP_{ND} in individual subjects at baseline and inhibition condition.

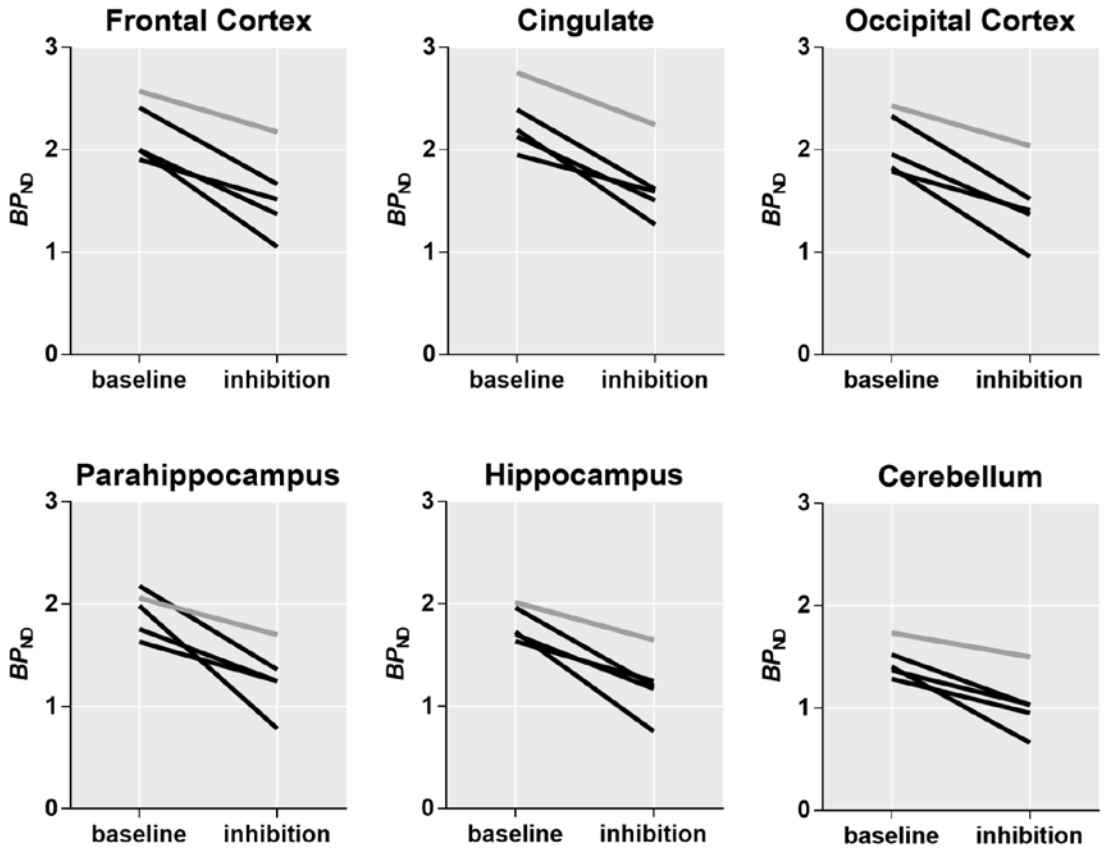

Fig. 4. B_{max} estimates

Average B_{max} across all regions (21 VOIs total) were computed from the known BP_{ND} estimates, the plasma concentration of DMXB-A and the receptor affinity, K_D, which was calculated as 0.35 nM based on known values from ^{125}I α–bungarotoxin *in vitro* studies. The analysis reveals that the average B_{max} across all regions ranged from 0.76-0.96 nM in the five subjects, and the K_i ranged from 170-385 nM.

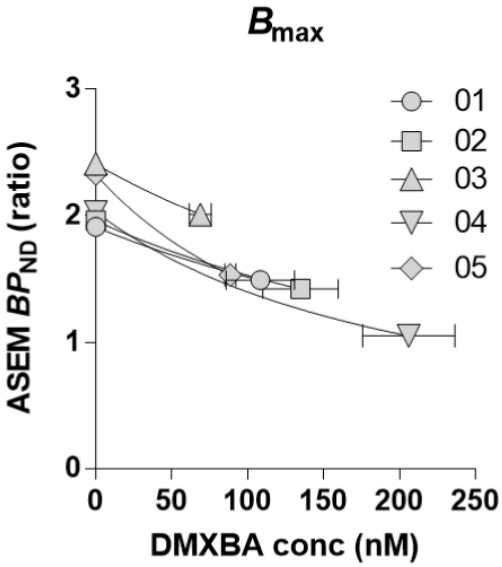

	01	02	03	04	05
Bmax	0.67	0.69	0.84	0.71	0.82
Kd	= 0.35	= 0.35	= 0.35	= 0.35	= 0.35
Ki	385	355	346	221	170

Fig 5. Distribution of V_T in healthy patients and controls
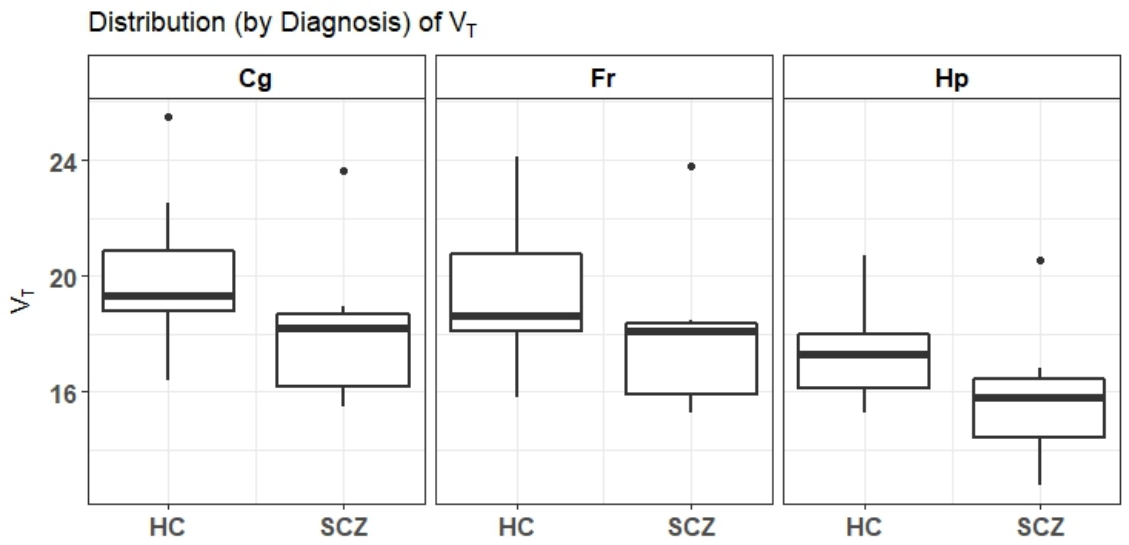
Boxplots of the distribution of V_T in healthy controls (HC) and patients with schizophrenia (SCZ), in Cingulate Cortex (Cg), Hippocampus (Hp), and Frontal Cortex (Fr). The single points above the limits of the boxplot are outliers.